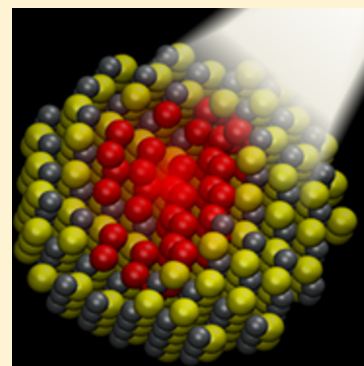


# Plasmon Resonances of Semiconductor Nanocrystals: Physical Principles and New Opportunities

Jacob A. Fauchaux,<sup>†</sup> Alexandria L. D. Stanton,<sup>†</sup> and Prashant K. Jain<sup>\*,†,‡,§</sup>

<sup>†</sup>Department of Chemistry, <sup>‡</sup>Materials Research Lab, and <sup>§</sup>Department of Physics, University of Illinois Urbana–Champaign, Urbana, Illinois 61801, United States

**ABSTRACT:** The discovery of localized surface plasmon resonances (LSPRs) in doped semiconductor nanocrystals has opened a new regime in plasmonics. We address both the technological and fundamental advances made possible by the realization of LSPRs in semiconductor nanocrystals. LSPRs were originally thought to be specific only to metallic nanostructures, but since their manifestation in semiconductor nanostructures, LSPRs are being seen as ubiquitous optical signatures of charge carriers. As fingerprints of a charge carrier collection, LSPRs of semiconductors are emerging as optical probes of processes that involve carrier dynamics, including redox reactions, electrochemistry, phase transitions, and photocatalysis. Unlike their electrical counterparts, LSPRs allow remote contactless probing and minimal device design. Ultrasmall semiconductor quantum dots are now enabling access to plasmon resonances of a handful of charge carriers, allowing us to ask fundamental questions regarding the lower limit of charge carriers needed to sustain a plasmon resonance, the emergence of a collective mode from a single-electron transition, and the effect of quantum confinement on plasmon resonances. These fundamental issues are discussed here, along with the need for new physical models required to capture the unique aspects of semiconductor LSPRs.



Localized surface plasmon resonances (LSPRs) in noble metal nanoparticles have been studied over the last few decades due to their ability to fundamentally alter light–matter interactions and their potential applications in enhanced spectroscopies,<sup>1–4</sup> sensing,<sup>5,6</sup> photocatalysis,<sup>7</sup> and optical devices.<sup>8</sup> However, recently, a new regime in plasmonics has opened up due to the discovery of LSPRs in nanocrystals of the semiconductor Cu<sub>2–x</sub>S.<sup>9–11</sup> Cu<sub>2–x</sub>S can support multiple copper-deficient stoichiometries that are naturally heavily p-doped, giving rise to hole carrier concentrations capable of sustaining a LSPR in the near-infrared (NIR). This NIR LSPR shares many attributes with the visible-range LSPRs of noble metals. Metal-like LSPRs have since been found in a variety of semiconductor nanocrystal systems, including copper selenide,<sup>12,13</sup> tungsten oxide,<sup>14</sup> indium oxide,<sup>15</sup> copper telluride,<sup>16,17</sup> germanium telluride,<sup>18</sup> and zinc oxide.<sup>19–21</sup>

Recent findings raise fundamental questions about the possibly unique nature of LSPRs in non-metallic nanostructures and even about the physical nature of the LSPR phenomenon itself.

On one hand, these recent findings are seen as an extension of nanoplasmonics to materials beyond the traditional noble metal coterie of gold, silver, and copper and to frequency domains outside of the visible spectrum. However, on the other, these findings raise fundamental questions about the

possibly unique nature of LSPRs in nonmetallic nanostructures and even about the physical nature of the LSPR phenomenon itself. With the discovery, LSPRs are no longer seen as just attributes of metal nanostructures; rather, they are being recognized more generally as optical signatures of any nanoscale collection of charge carriers. These “new” LSPRs can be employed for exploring poorly understood physics of charge carrier interactions, nanoscale probing of chemical processes involving charge dynamics, and developing actively tunable optoelectronic devices. This Perspective addresses the exciting fundamental and technological opportunities arising from the newly found plasmon resonances of semiconductor nanocrystals.

*A New Form of Control.* It is known that the LSPR spectra of noble metal nanoparticles can be tuned by variation of the size, shape, composition, or dielectric environment of the nanoparticles.<sup>22–25</sup> However, metals lack a particular type of tunability that is offered only by semiconductors, that is, through a change in the free carrier concentration, a physical parameter that determines the square of the LSPR frequency, as described by the Drude model. Carrier densities in noble metals like gold and silver are large ( $\sim 10^{23}$  cm<sup>−3</sup>) and difficult to change appreciably, although small shifts in the LSPR frequency originating from charging/discharging of a metal nanoparticle have been reported.<sup>26,27</sup> In contrast, semiconductors have carrier densities that can be varied from  $10^{16}$  to  $10^{21}$  cm<sup>−3</sup>, most commonly by means of electronic doping.<sup>28,29</sup> In a nanocrystal

**Received:** January 7, 2014

**Accepted:** February 27, 2014

**Published:** February 27, 2014

(say,  $\sim 5$  nm in diameter), the addition of tens of carriers allows one to span this wide range of carrier densities (Figure 1).

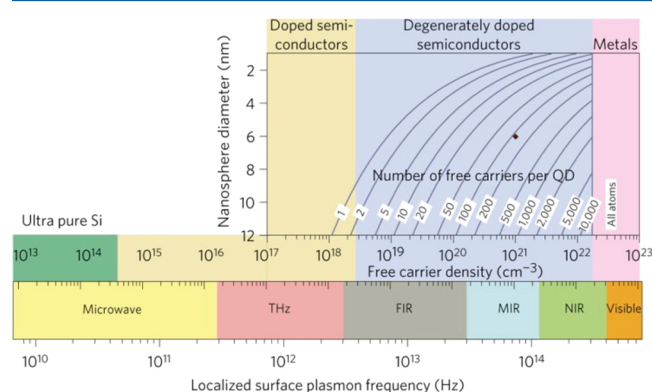


**Figure 1.** A two-dimensional plot based on the Drude model shows the LSPR frequency as a function of the diameter of the nanocrystal (y-axis) and the number of free carriers (contour lines), illustrating the wide range of LSPR frequencies accessible by control of the carrier density of a semiconductor nanocrystal. Reproduced with permission from ref 10. Copyright 2011, Nature Publishing Group.

Consequently, LSPRs of semiconductor nanocrystals can be tuned from the terahertz (THz) regime to NIR frequencies, as long as controlled doping is achievable, either via the creation of intrinsic defects (see the example of  $\text{Cu}_{2-x}\text{S}$  nanocrystals in Figure 2) or the addition of extrinsic impurities. It is encouraging that the community has already identified a number of such semiconductors (e.g., copper sulfide,<sup>3,30</sup> copper selenide,<sup>12</sup> and copper telluride<sup>16</sup>) that allow controlled

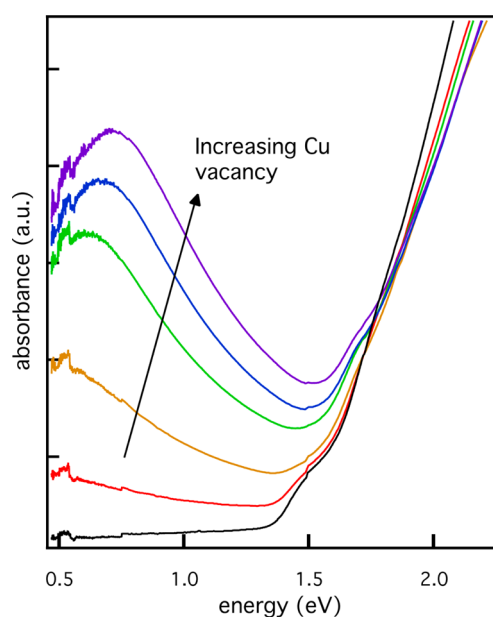


**Figure 2.**  $\text{Cu}_{2-x}\text{S}$  nanocrystals display a LSPR that is tunable by control of the vacancy density within the nanocrystal. Fully stoichiometric  $\text{Cu}_2\text{S}$  nanocrystals show no LSPR absorption, but exposure to oxygen leads to the formation of Cu vacancies in the lattice and the onset of a LSPR in the NIR region. Further exposure to oxygen creates more Cu vacancies, leading to an increase in strength and a blue shift of the LSPR band, consistent with an increase in carrier density. Reproduced with permission from ref 10. Copyright 2011, Nature Publishing Group.

electronic doping to levels as high as a few hundred carriers per nanocrystal.

**Dynamic Tunability of Optical Resonances.** Metallic nanostructure LSPRs cannot match the large dynamic range of electro-optically tunable semiconductor nanocrystal LSPRs. There is yet another distinction. The tunability of metal nanostructure LSPRs is static in nature; a metal nanostructure can be synthesized with a desired LSPR frequency by appropriate choice of the size, shape, and/or composition of the nanostructure. However, once designed, the LSPR spectrum is largely fixed, and postsynthetic variation is not possible. In contrast, semiconductor nanocrystals offer a dynamic form of LSPR tunability; the carrier concentration of an already synthesized nanocrystal can be varied in situ by redox doping or electrochemical means,<sup>30,31</sup> allowing the LSPR spectrum of the nanocrystal sample to be tuned on the fly. Such active control combined with the large dynamic range of the tunability makes complete on/off switching of LSPRs possible (Figure 3). The achievement of optical switching gives rise to

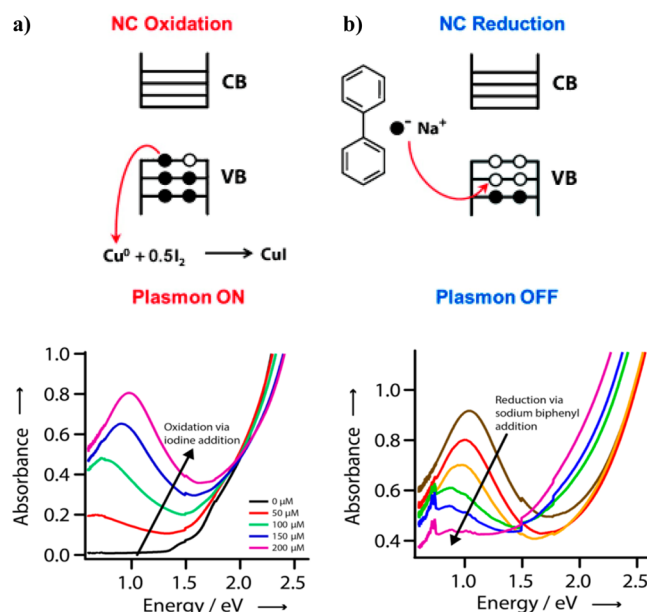


**Figure 3.** On/off control of semiconductor nanocrystal LSPRs. (a) Exposure of cuprous sulfide nanocrystals to oxidants such as iodine causes the formation of Cu vacancies and holes in the valence band, resulting in switching on of the LSPR. (b) Exposure to reducing agents such as sodium biphenyl causes filling of the Cu vacancies, resulting in switching off of the LSPR. Adapted with permission from ref 30. Copyright 2013, Wiley-VCH Publishers, Inc.

remarkable opportunities in the field of photonics, quite analogous to the revolution brought about in electronics by the development of the electronic switch, that is, the transistor. The electronics industry relies on the dynamic on-chip tunability of the electronic conductivity of a semiconductor. Switches, transistors, and modulators require dynamic control of electronic conductivity, making it unsuitable to use metals, which have conductivities that are largely invariant. Similarly, active circuit elements for photonics cannot be based on metal nanoparticles with static LSPRs. Semiconductor nanocrystals, with dynamically tunable plasmon resonances, present the much needed building blocks for active photonic circuits. There is an opportunity to use these nanocrystals for fabrication of

optical analogues of transistors and logic gates and thereby advance the field of photonics.

*Sensitivity Down to Singular or Quantized Events.* There has been significant discussion of the sensitivity of LSPR tunability of metal nanostructures.<sup>32–35</sup> It is worth commenting on the electro-optic sensitivity of semiconductor nanocrystal LSPRs, which follows one very simple physical relationship; the smaller the nanocrystal, the more sensitive the LSPR frequency to changes in the number of free carriers because for a given number of charges, the change in carrier density for a smaller nanocrystal is greater. In theory, the electro-optic sensitivity goes as  $1/r^3$ , where  $r$  is the radius of the nanocrystal.

**LSPRs are no longer seen as just attributes of metal nanostructures; rather, they are being recognized more generally as optical signatures of any nano-scale collection of charge carriers.**

By employing ultrasmall nanocrystals, one can achieve an unprecedented level of sensitivity. For instance, the addition of a single carrier to a 3 nm nanocrystal results in an increase in the carrier concentration by  $10^{20} \text{ cm}^{-3}$ , large enough to cause an easily detected  $\sim 100 \text{ nm}$  shift in the LSPR wavelength of a NIR resonance. The implications are huge; a single defect or impurity center formed within a nanocrystal can now be detected optically, or one can envision an electro-optic transistor with on/off control achieved by moving a single charge. However, before such promises can be realized, LSPRs in ultrasmall nanocrystals must be characterized in detail. In particular, it must be verified that the size of the nanocrystal does not jeopardize the sustenance of a high-enough-quality tunable plasmon resonance. Broadening of the LSPR due to surface scattering of charge carriers is expected to be one potential bottleneck. Quantum size effects may also complicate the collective nature of the plasmon resonance. A primary technical challenge to be addressed is the difficulty of single-nanocrystal-level detection in the NIR, which is still a nascent area. Significant improvement in the quantum yield and S/N of NIR detectors is desired, although promising work is being carried out in this new area.

*Plasmons Sustained by Small Numbers of Carriers.* Plasmons are collective excitations of a sea of carriers. There has always been curiosity about what happens to such a collective excitation when the “sea” contains a very small number of carriers. In a metal, each atom contributes a fixed number of electrons, typically one or two, depending on its valence. Thus, by decreasing the size of the nanoparticle to the few-atom cluster regime, LSPRs of a low number of carriers (few tens to a hundred) can be accessed. A classic example is the  $\text{Hg}_6^+$  cluster, which contains 11 electrons and exhibits a plasmon-like feature.<sup>36</sup> With a metal, however, it is not possible to tune the number of carriers in the nanoparticle independent of the nanoparticle size. As a result, the effects resulting from a very low number of carriers are convoluted with the effect of strong quantum size confinement of carriers.<sup>37–39</sup> Semiconductor nanocrystal LSPRs are advantageous in this regard because nanocrystal size and the number of carriers in a nanocrystal can be tuned independent of one another. It is possible, at a fixed nanocrystal size, to add or remove carriers and study the

evolution of the collective resonance purely as a function of the number of interacting charge carriers. For carrier concentrations of  $10^{20}$ – $10^{21} \text{ cm}^{-3}$  (which result in a LSPR in the easily accessible  $2 \mu\text{m}$  wavelength region), a 3-nm nanocrystal can hold fewer than 10 carriers. In fact, our lab exploited this fact in 3 nm ZnO nanoparticles<sup>19</sup> to show that a LSPR can be exhibited by as few as 4–5 electrons per nanocrystal, the lowest number of carriers reported thus far and much smaller than the  $\text{Hg}_6^+$  cluster. The finding that the sustenance of a LSPR needs much fewer carriers than conventionally thought does raise some fundamental questions, some of which are addressed later in this Perspective, but are in need of more detailed investigation:

(i) How is the physical nature of the plasmon resonance fundamentally different at a low number of carriers?

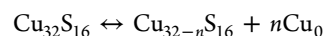
(ii) At what number of charge carriers is it no longer possible to observe a collective resonance?

(iii) As one increases the number of charge carriers, at what point do single-carrier intraband excitations give way to a collective plasmon resonance? What is the nature of this evolution? Do both single-carrier transitions and plasmon resonances coexist? How does one distinguish between the two excitations?

Some of these questions are addressed in recent work from Gamelin illustrating deviations from the Drude model in small ZnO nanocrystals.<sup>21</sup> An extended theoretical discussion is forthcoming from our group.

*Plasmons as Ubiquitous Signatures of Charge Carriers.* For the last several decades, LSPRs have been viewed simply as optical attributes of noble metal nanoparticles. However, this view is undergoing a paradigm shift with the finding of LSPRs in semiconductor and oxide nanocrystals; the LSPR is now being seen as a dynamic optical signature of the free carrier density within a nanocrystal. This new view has taken on a whole new meaning with the recent finding that even a handful of carriers, as small as four in number, can sustain a LSPR mode. Essentially, the LSPR can be considered, in the most general sense, as an optical signature of any arbitrary collection of charge carriers. It is not even essential for these charges to have purely free character.<sup>16,21</sup> With this new generalized view, it is clear to see the utility of the LSPR as a ubiquitous probe of chemical and electronic processes that involve carrier dynamics.

(i) *Redox Chemistry.* LSPRs of noble metal nanoparticles have been used for sensing quite extensively. In this case, one exploits the sensitivity of the LSPR frequency to changes in the refractive index of the local environment as per the resonance condition  $\epsilon_r(\omega) = -2n_m^2$ . Analytes, which induce a change in the local refractive index around the nanoparticle, are detected by shifts in the frequency of the LSPR band. The method is fairly limited; physical or chemical events, which do not involve a large enough change in refractive index, go undetected. On the other hand, LSPRs of semiconductors, being highly sensitive to the carrier concentration, can be used for detection of electronic processes. A wide range of processes, in particular, redox chemistry, thus becomes accessible. Cuprous sulfide is particularly sensitive toward redox and electrochemistry, as summarized by its reaction



Oxidizing environments and/or potentials favor the forward reaction involving the formation of Cu vacancies and valence band holes in the nanocrystal, thereby resulting in an increase in the intensity and a blue shift of its LSPR. Reducing



conditions result in filling of the formed vacancies via the backward reaction, leading to a red shift and a decrease in the intensity of the LSPR. The action of common redox agents such as  $I_2$  and sodium biphenyl has been detected using this approach.<sup>30</sup> Resolution of the role of common ligands, such as amines and thiols, as p- or n-type electronic dopants was also possible. This approach may allow the sensing of nanoscale fields and voltages in the near future.

Conventionally, electronic processes are detected by means of electrical transport measurements on nanoparticles. Such measurements suffer from many disadvantages, a primary one being that a thin-film-type electrical device must first be constructed. Electrical contacts can significantly alter the measured signal, and interparticle charge hopping can dominate the signal,<sup>40</sup> thereby obscuring the carrier changes occurring within a nanoparticle. The ability to carry out measurements in solution in real time in a remote contactless manner is a distinct advantage of using LSPRs as a probe.

(ii) *Photoelectrochemistry*. Photocatalysis involves the dynamic generation, transfer, and electrochemical utilization of photoexcited electrons and holes, processes that are typically difficult to monitor. LSPRs are proving to be a useful tool for detecting such photoprocesses.<sup>26</sup> For instance, ZnO nanoparticles when irradiated with UV light under anaerobic conditions exhibit a buildup of photoexcited electrons in the conduction band.<sup>41–43</sup> This charge buildup is detected via the emergence of a LSPR absorption band in the NIR region. The frequency of the LSPR band, that is,  $\sim 0.55$  eV, can be used as a measure of the number of charges in the conduction band. Upon exposure of these photocharged nanoparticles to reactants like oxygen or resazurin (Figure 4), the electrons are utilized for a surface redox reaction, which is detected via a red shift and decrease in the intensity of the LSPR band. From the magnitude of the LSPR shift, the number of reaction turnovers occurring on a nanoparticle is quantifiable.

Such optical sensing of photogenerated carriers can be particularly useful in metal/oxide heterostructures. Much attention has focused on composites of plasmonic noble metal nanoparticles and semiconductor oxide nanoparticles, which display enhanced photocatalytic activity under plasmonic excitation. Injection of plasmonically generated carriers from the metal to the semiconductor has been proposed as a probable mechanism of photoactivity.<sup>44–46</sup> IR LSPRs arising from conduction band carriers in the semiconductor nanoparticle would offer definitive proof of charge injection in these systems and help elucidate the nature of charge transfer, in turn aiding the development of heterostructures optimized for photocatalysis. The fact that no more than a few charge carriers are needed to sustain an IR LSPR in small semiconductor nanoparticles is particularly useful in this regard.

(iii) *Sensing of Crystallographic Phase*. Information about the crystallographic phase of a solid-state material is most often obtained through electron or X-ray diffraction, making real time detection of a phase transition in realistic environmental conditions difficult. Optical signatures of phase, on the other hand, can allow real time monitoring of phase transitions under ambient conditions and with minimal perturbation. LSPRs could be promising as such optical signatures. While not yet a general finding, in the specific case of GeTe nanoparticles, the LSPR has been shown to be sensitive to the crystalline nature of the material. GeTe is a semiconductor with a high density of cationic vacancies and consequently hole concentrations on the order of  $10^{21} \text{ cm}^{-3}$ . Consistent with this fact, crystalline GeTe

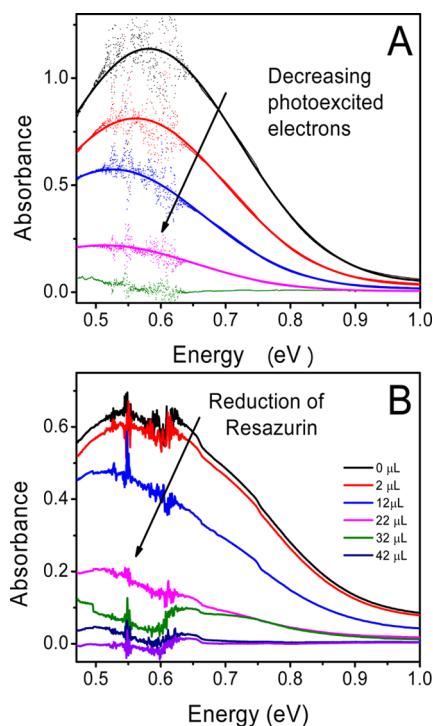


**Figure 4.** LSPR-based quantitative detection of photogenerated electrons in ZnO nanocrystals. Photogenerated electrons are utilized in surface redox reactions with oxygen (A) or resazurin (B), detected via a decrease in intensity and a red shift of the LSPR absorption band, consistent with a reduction in the photogenerated electron concentration. Reproduced with permission from ref 19. Copyright 2013, American Chemical Society.

nanoparticles exhibit a strong LSPR band centered at  $\sim 0.5$  eV (Figure 5c), in agreement with predictions from a modified Drude model (Figure 5d). Amorphous GeTe nanoparticles, on the other hand, display only a band gap absorption onset at about 0.3 eV (Figure 5a). The LSPR feature is absent, likely due to the strong localization of free carriers by the high density of midgap defects in the amorphous phase. When the amorphous nanoparticles are subject to crystallization, the LSPR feature is switched on. The LSPR absorption band thus becomes a facile probe of the amorphous-to-crystalline transition, in the absence of which high-resolution transmission electron microscopy (HRTEM) or diffraction would be necessary to distinguish the two phases. Phase-sensitive LSPRs may open up the possibility of optically detecting phase transitions on single nanocrystals or performing time-resolved optical pump–probe studies of phase transitions. Such studies can provide new insight into the microscopic dynamics of phase transitions frequently smeared out by ensemble averaging. Phase-switchable LSPRs may also have applications in optical data storage and photonic switches.

(iv) *Carrier Gas Phenomena*. A LSPR is an optical signature of a free carrier gas, which can be formed or disrupted in phenomena such as Mott insulator-to-metal transition and Anderson localization. The LSPR can thus be useful for detecting such phenomena. For instance, in small ZnO nanoparticles, the LSPR generated upon photocharging is an indicator that a free-electron gas is formed upon photoexcitation of enough electrons into the conduction band. From the LSPR frequency, it is deduced that the excess electron concentration is  $\sim 4 \times 10^{20} \text{ cm}^{-3}$ , well above the suggested Mott density ( $6 \times 10^{18} \text{ cm}^{-3}$ ) of ZnO. Consistent with the

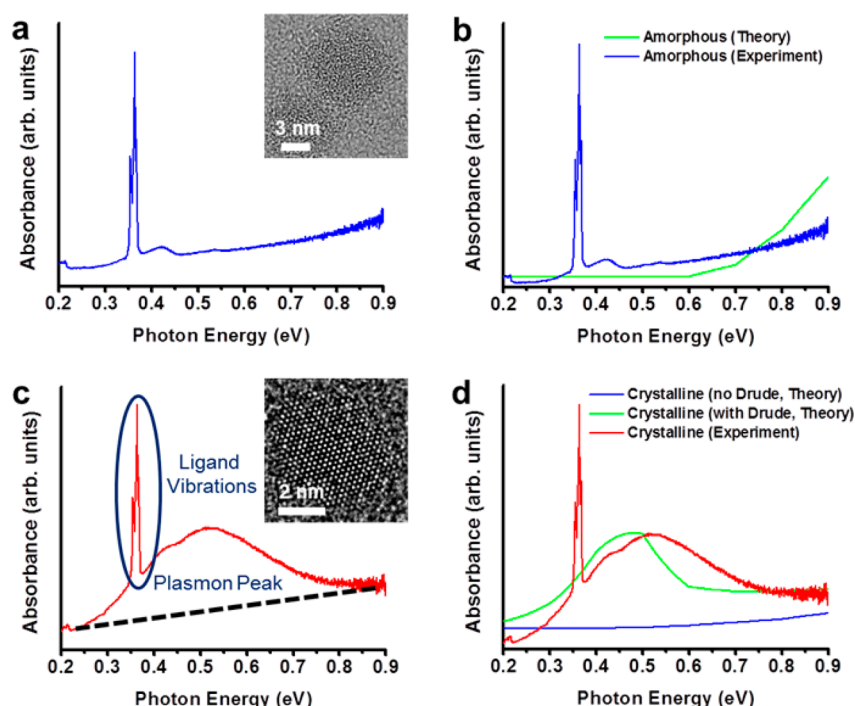


**Figure 5.** LSPR as a signature of the crystallographic phase. Absorption spectra (a,c) show that crystalline GeTe nanoparticles (c) exhibit a LSPR centered at  $\sim 0.5$  eV, whereas the amorphous nanoparticles (a) lack such a resonance. HRTEM images of a representative nanoparticle are shown in the inset. Comparison of experimental and calculated absorption spectra of amorphous (b) and crystalline (d) GeTe nanoparticles shows good agreement. Reprinted from ref 18. Copyright 2013, American Physical Society.

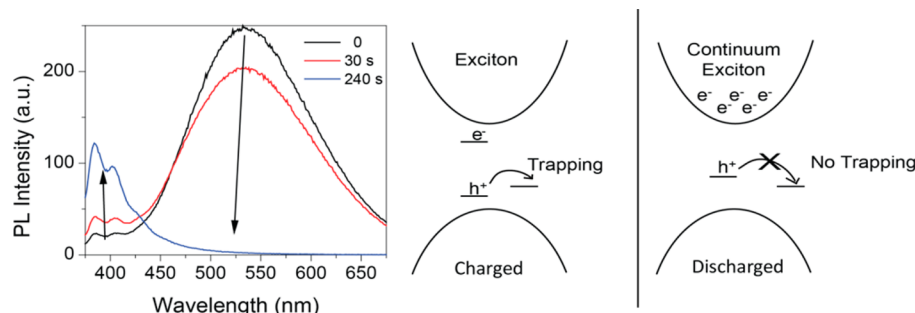


**Figure 6.** Upon UV photocharging of ZnO nanocrystals, the defect photoluminescence is completely shut off, and concomitantly, the band edge photoluminescence is enhanced (left). The observation of a LSPR band confirms that a free-electron gas is formed in photocharged ZnO. This free-electron gas solvates any hole formed by further photoexcitation (right). Consequently, the hole is much more stable against trapping by surface defects, resulting in the suppression of defect photoluminescence and the enhancement of band gap photoluminescence. Reprinted with permission from ref 19. Copyright 2013, American Chemical Society.

formation of a free-electron plasma, the charged state exhibits high dielectric screening, under which bound electron–hole excitonic states cannot be sustained. This phenomenon explains why the excitonic band is bleached in the charged state of ZnO nanoparticles, a well-known occurrence.<sup>41,43</sup> In addition, the free-electron gas solvates any hole formed by further photoexcitation through Coulomb interactions. This multicarrier state is known as a continuum or Mahan exciton. The resulting stabilization of the hole greatly reduces the possibility of trapping of this hole by surface defects. This explains why defect photoluminescence is suppressed in charged ZnO nanoparticles (Figure 6), another oft-observed phenomenon.<sup>47,48</sup> Thus, the confirmation of a free-electron gas by means of the LSPR turned out to be useful in addressing two long-standing yet unresolved observations. Previous proposals could not explain both of these observations consistently.

*Assignment of Spectral Bands to LSPR Modes.* With semiconductor nanocrystals, it is often necessary to have a method for unambiguous assignment of a spectral feature to a LSPR mode. This need arises from multiple factors:

(i) Unlike the well-established field of noble metal nanoparticle plasmonics, reports of semiconductor nanocrystal LSPRs are more recent. In the case of many semiconductors, the finding of LSPRs is being made for the first time. Some degree of doubt or uncertainty is warranted.

(ii) The position and intensity of the LSPR band is sensitive to the carrier or dopant density within the nanocrystals, which can vary dramatically depending on synthesis or postsynthetic conditions, leading to some uncertainty about a LSPR assignment. There can also be variation in spectra from one sample to another, despite uniform conditions of synthesis or processing.

(iii) Even if the carrier concentration is known (through a separate analysis), a LSPR assignment can be difficult. The Drude free carrier model, which is quite useful in the case of noble metal nanoparticles for deducing LSPR peak positions from carrier concentrations, can deviate significantly for semiconductor nanocrystals. This is discussed in detail in the next section. In addition, reliable values of the effective masses of carriers and high-frequency dielectric constants may not always be available for a given semiconductor.

(iv) Optical absorbance spectra of semiconductor nanocrystals are more complex when compared to those of noble metal nanoparticles. Apart from LSPR modes, sub-band gap absorption features originating from single-electron intraband transitions, electronic transitions into midgap or defect states, phonons, ligand, and solvent vibrations dominate the spectrum. This is especially true in the IR region. In particular, single-electron intraband transitions and LSPRs can be difficult to distinguish from one another because of their similar origin; they both result from excess electrons (holes) in the conduction (valence) band. This lack of distinction can be a source of debate, unless specific tests or methods exist for the purpose of assigning an observed spectral band to a LSPR or otherwise.

We analyze some commonly used methods for making LSPR assignments.

It is clear to see the utility of the LSPR as a ubiquitous probe of chemical and electronic processes that involve carrier dynamics.

(i) *Size Dependence.* Researchers working in the field of nanoparticles often invoke size dependence as a defining feature of a LSPR mode. However, size dependence can be complicated, especially in the case of semiconductor nanocrystals. It is known from noble metal nanoparticles that in the 20–100 nm size regime, larger nanoparticles generally have a red-shifted LSPR band due to the effect of retardation and radiative damping. The red shift is however small and can be obscured by spectral broadening from nanoparticle heterogeneity. Also, semiconductor nanocrystals studied are rarely in this size regime. Below the 20 nm size, the quasi-static dipolar limit applies, and the LSPR frequency is expected to be size-independent. However, once the nanoparticle size becomes much smaller than the mean free path length of carriers, surface scattering of electrons results in a significant broadening and a slight red shift of the LSPR. While the latter effect is potentially useful as a test, one must be aware that this effect is convoluted with quantum size effects, whereby confinement of carriers results in a significant modification of the dielectric function and a blue shift of the LSPR.<sup>37,38</sup> For metal nanoparticles, such quantum size effects are operative below 1–2 nm; however, in semiconductors, de Broglie wavelengths of free carriers are much larger, and quantum size effects can be operative in the ~5 nm regime, which is a common size scale for semiconductor nanocrystals being studied in the field of plasmonics. Another factor that can complicate size-dependent trends is a potential variation in doping levels for nanocrystals of different size, resulting from a perturbation of the electronic structure. Without verifying that different size samples all reach identical

carrier concentrations, analysis of size trends is meaningless. Effective masses of carriers can also show some variation with size, significantly influencing LSPR frequency positions.

(ii) *Sensitivity to the Medium Refractive Index.* Another defining signature of a LSPR is the sensitivity of the resonance frequency to the medium dielectric constant or refractive index, which was employed in an early study.<sup>10</sup> Typically, the nanoparticles are dispersed in solvents of varying refractive indices; the higher the refractive index of the medium, the more red-shifted the LSPR. The red shift expected from an increase in the refractive index of the solvent by 0.2 units is about 10–15 nm under ideal conditions. However, the sensitivity of a plasmonic nanoparticle has been shown to fall off significantly at a distance equal to about 1/5th of the diameter of the nanoparticle.<sup>49</sup> For small semiconductor nanocrystals, this means that the ligand environment dominates the effective medium experienced by the nanocrystal, thereby diluting any refractive index changes that result from a change in the solvent. Such shifts are therefore difficult to reliably detect, especially in the presence of significant broadening of LSPR bands. The choice of solvents is also fairly limited considering that they must be both significantly different in refractive index from one another and also non-IR absorbing, CCl<sub>4</sub>, CS<sub>2</sub>, and tetrachloroethylene being one possible set of solvents of significantly different refractive index. In some cases, certain solvents are unable to disperse the colloidal nanocrystals, or they may adversely affect the ability to dope or charge the nanocrystals.

(iii) *Variation of Carrier Concentration.* A more definitive test of a LSPR is the variation of the resonance frequency as a function of carrier concentration, which is useful in cases where a systematic variation of doping/carrier density is possible. A LSPR band is expected to blue shift and increase in intensity upon an increase in carrier concentration. Likewise, the band will be suppressed and red-shifted as the carrier concentration is decreased. A band resulting from single-electron intraband transitions is not expected to necessarily follow such a trend because the energy of such transitions is dictated by the details of energy spacing between conduction (or valence) band levels. Even if the Drude model of free carriers is not strictly valid, one can expect the LSPR frequency to change approximately as the square root of the carrier concentration and the intensity to vary in direct proportion to the carrier concentration. Of course, for verifying such a trend, an analytical measure of the carrier concentration is needed, often achieved by elemental analysis, through electrical measurements, or through titration against mild redox agents.

(iv) *Interparticle Coupling.* A considerably more reliable test is based on interparticle coupling, as exploited in a recent study from our group.<sup>19</sup> It is well-known from assemblies of silver and gold nanoparticles<sup>50</sup> that when (spherical) plasmonic nanoparticles are brought into close proximity of one another, the LSPR exhibits large (up to a few hundreds of nanometers) red shifts<sup>51</sup> due to the electromagnetic coupling of plasmon resonances on nearby nanoparticles. As long as a controllable method for colloidal aggregation or assembly of nanoparticles is available, this test can be utilized with ease.

(v) *Shape or Anisotropy Effects.* Another conclusive test involves the study of anisotropic nanoparticles, provided such shape control is possible.<sup>52,53</sup> Anisotropic nanoparticles are expected to show separate LSPR modes for each unique axis. Shape or anisotropy parameters (e.g., aspect ratio for rod-shaped nanoparticles) can be used to predict the relative energy



positions of the LSPR modes by use of Gans theory. There is however one caveat; the effective mass of carriers can be different along each axis, which compromises the value of such predictions.<sup>16</sup> It has also been shown that in semiconductor nanorods of high aspect ratio, charge carriers can be significantly localized, preventing their free mobility along the long axis, which can disrupt the sustenance of a long-axis LSPR mode. For low aspect ratio rods, short-axis and long-axis LSPR modes may be too poorly separated in energy to be resolved. It is possible that these limitations are valid only in specific semiconductor systems,<sup>16</sup> and in general, shape effects are possibly useful tests of LSPR assignments.

A combination of tests described above can often result in an unambiguous LSPR assignment.

*Are New Physical Models Needed For Semiconductor Nanoplasmonics?* The Drude free-electron model is used to describe quite satisfactorily noble metal nanoparticle LSPRs. Is a sufficiently different model needed to fit LSPR spectra of semiconductor nanocrystals? Addressing this question will allow quantitative prediction of LSPRs in semiconductors and also provide insight into if and how the physical nature of LSPRs is significantly different in semiconductor nanocrystals as compared to that for noble metal nanoparticles. For sufficiently large nanocrystals (size  $\gg$  de Broglie wavelength of the carrier) and a sufficiently large number of carriers, a Drude treatment of the collective resonance is valid, with some modifications that are standard in solid-state physics. The only consideration that one must make is that the carriers involved in the collective resonance can be either conduction band electrons or valence band holes, and parameters for the appropriate carrier type must be used.

(i) *Effect of Band Gap Transitions.* There is a need to include the effect of band-to-band transitions on the dielectric response. This is particularly important when there is significant overlap between the band gap energy and the LSPR energy, resulting in coupling of these two transitions. This is done through the addition of a bound electron contribution  $\epsilon_{\text{bound}}(\omega)$  to the Drude free carrier response as

$$\epsilon(\omega) = \epsilon_{\text{bound}}(\omega) - \frac{\omega_p^2}{\omega^2 + i\omega\gamma} \quad (1)$$

Here,  $\omega_p$  is the plasma frequency

$$\omega_p = \frac{Ne^2}{m_e\epsilon_0} \quad (2)$$

where  $N$  is the carrier concentration,  $e$  is the electronic charge,  $m_e$  is the effective mass,  $\epsilon_0$  is the permittivity of free space, and  $\gamma$  is bulk collision frequency of carriers. It must be noted that the inclusion of the contribution of interband transitions is not unique to semiconductors. Similar corrections to the Drude model are applied for noble metals. For instance, in the case of gold,  $d \rightarrow sp$  transitions overlap significantly with LSPRs of spherical nanoparticles, resulting in a significant broadening, red shift, and damping of the LSPR, an effect that is modeled by including a frequency-dependent complex contribution of bound  $d$ -band electrons of gold. In cases where the LSPR energies are sufficiently far from interband transitions, simply adding a high-frequency dielectric constant ( $\epsilon_\infty$ ) to the Drude free carrier contribution suffices

$$\epsilon(\omega) = \epsilon_\infty - \frac{\omega_p^2}{\omega^2 + i\omega\gamma} \quad (3)$$

Because semiconductor LSPRs are often in the IR region, there can be significant energetic overlap with phonon modes as well as intraband transitions of electrons or transitions involving midgap or defect states. The contribution of these transitions must also be included via a complex frequency-dependent dielectric term.

(ii) *Localization of Carriers.* Carriers in a semiconductor do not have purely free character; rather, they show some degree of localization due to the preponderance of the periodic lattice potential. Carrier localization is probably the most critical effect that must be corrected for in the Drude free-carrier model. Typically, the effect of localization is treated phenomenologically through the use of an effective mass for the charge carriers, as shown in eq 2. After all, effective mass models are common approximations in semiconductor physics. A higher degree of localization is represented by a smaller effective mass, resulting in a larger bulk plasma frequency and a blue-shifted LSPR relative to the free carrier value. Values of carrier effective masses and high-frequency dielectric constants available from electrical measurements on bulk semiconductors may be used as long as the nanoparticle size is not too small so as to significantly perturb the electronic structure of the semiconductor. The electronic structure and consequently effective masses and high-frequency dielectric constants may also vary significantly with heavy doping (e.g., in  $\text{Cu}_{2-x}\text{S}$ , literature values of  $\epsilon_\infty$  range from approximately 3 to 10). In anisotropic lattices, the effective mass, a tensor quantity, can also be different along different crystal axes. In less straightforward cases, ab initio approaches may be needed for calculating the dielectric function, taking into account the specific details of the doping level, anisotropy, and the crystallite size.

(iii) *Ligand and Proximal Effects.* The effect of the ligand shell also needs to be considered.<sup>54</sup> Although ligand effects are frequently considered for metal nanoparticles, these are typically modeled as nonresonant effects by means of a frequency-independent medium dielectric constant. This approximation is valid for typical nonchromophoric ligands in the visible regime; however, in the case of semiconductor LSPR modes, which lie in the IR region, there can be significant spectral overlap with ligand and solvent vibrational overtones.<sup>55</sup> The resulting resonant interaction needs to be incorporated through use of a complex frequency-dependent dielectric term for each ligand and solvent vibrational resonance. The effect can range from a small perturbation of the LSPR spectrum to strong coupling effects such as hybridization of modes and Fano interference, similar to what has been seen in hybrids of plasmonic metal nanoparticles and chromophores.<sup>56,57</sup> In the case of assemblies and aggregates of nanoparticles, electrodynamic coupling of LSPR modes of vicinal nanoparticles needs to be considered, not unlike noble metal nanoparticles. Interparticle coupling can shift LSPR bands quite considerably and result in enhancement of multipolar resonances. Electrodynamic simulation methods like finite difference time domain and discrete dipole approximation can be useful for modeling these effects, as long as there is reasonable knowledge of interparticle distances and assembly configuration.

(iv) *Small Size Regime.* One effect of small size is well-known from Kriebig's work on noble metal nanoparticles. When the size is much smaller than the mean free path of carriers, there is significant scattering of carriers with the nanoparticle surface.

Surface scattering needs to be included via modification of the bulk collision frequency  $\gamma_{\text{bulk}}$  as

$$\gamma = \gamma_{\text{bulk}} + \frac{A\nu_F}{R} \quad (4)$$

where  $\nu_F$  is the Fermi velocity of carriers,  $R$  is the radius of the particle, and  $A$  is a phenomenological parameter ranging from 0 to 1 describing the nature of surface scattering. Surface scattering results in significant broadening of the LSPR band and also a small red shift. The smaller the nanocrystal size, the greater these two effects on the LSPR band.

The implications are huge; a single defect or impurity center formed within a nanocrystal can now be detected optically, or one can envision an electro-optic transistor with on/off control achieved by moving a single charge.

However, another effect is considerably more important in the case of semiconductors. In small nanocrystals (ca. 10 nm and smaller), carriers experience quantum confinement. This size-dependent confinement not only increases the band gap but also raises the spacing between energy levels within the conduction and valence bands. The dielectric response of carriers within either band is perturbed as a result, which can be accurately deduced only by means of a quantum mechanical treatment involving carriers confined in a potential well. The effect of quantum confinement has been shown to result in a blue shift of the LSPR.<sup>37–39,58</sup> The smaller the size, the stronger this confinement, and the greater the LSPR shift relative to the large size limit. However, at extremely small sizes, the energy level spacing can increase to an extent such that it is much greater than the bulk plasma frequency, which is a measure of Coulomb interaction between carriers. This occurrence would effectively disrupt the sustenance of a collective resonance of carriers. It must be noted that quantum confinement effects are operative in metal nanoparticles as well; however, these effects become important only in the cluster size (<1–2 nm) regime. In semiconductors, carrier concentrations are much lower (typically 10–100× smaller than that in metals); consequently, Fermi energies are smaller, and de Broglie wavelengths are much longer (~5 nm). As a result, the effect of confinement is considerable even at nanocrystal sizes as large as 5 nm. Metals on the other hand have much higher carrier concentrations, larger Fermi energies, and smaller de Broglie wavelengths.

(v) *Few Carriers.* Resonances sustained by an extremely small number of carriers can have significantly different character compared to resonances involving hundreds of carriers (classical limit). In the limit of a single carrier, only single-carrier intraband transitions are possible; collective resonances do not exist. As the number of carriers is increased, Coulombic interactions between carriers become increasingly important, and a collective resonance begins to emerge, and concomitantly, the relative contribution of single-carrier transitions decreases. In this intermediate regime, a quantum mechanical treatment of a collection of a discrete number of carriers in a confined potential becomes necessary to describe the dielectric

response and the collective nature of the LSPR. Electron–electron correlations may also need to be included for accuracy. In this intermediate regime, carriers involved in a collective resonance have an additional degree of bound character, the dielectric response of which is closer to that of a bound Lorentz oscillator model rather than the pure Drude oscillator. These theoretical considerations are necessary for accurate modeling of the nature of the collective resonance in few-carrier systems and also for understanding how a collective resonance evolves from single-carrier transitions.

Thus, a number of specific opportunities exist in the growing field of semiconductor nanocrystal plasmonics. The search for LSPRs in previously unexplored semiconductor systems will likely continue. These findings will expand the library of systems that support LSPRs and will also make LSPRs truly ubiquitous in solid-state nanoscience. Control over carrier/dopant concentrations and consequently over LSPR spectra has been achieved only for a few semiconductors, in particular, the copper chalcogenides. In other materials, physical and chemical methods for systematic control need to be explored. Even in the case of copper chalcogenides, the reproducibility and stability of the stoichiometric composition and the resulting LSPR spectrum have yet to be established. On the fundamental front, several questions, especially those related to the physical nature of few-carrier LSPRs, quantum confinement effects, and carrier–carrier correlations, deserve detailed experimental and theoretical investigation. It is encouraging to see that some work in this area has already been initiated. The field is also in need of quantitative rigor. Many early studies, including those from our group, were mostly qualitative in nature, one example being the redox sensing demonstrations. The rendering of LSPRs as optical signatures of a free carrier gas or a solid-state phase, while exciting, is thus far limited to very specific cases; there is no doubt that this idea needs to be demonstrated to be more general and thereafter exploited for addressing complex questions in solid-state physics. While LSPRs of noble metal nanoparticles are routinely studied and exploited on the level of individual nanoparticles, this Perspective points out the huge opportunity for single-particle studies in the case of plasmonic semiconductor nanocrystals, especially for quantum sensing and electro-optic switching. Likewise, we tout some novel photonic applications of the active plasmons of semiconductor nanocrystals, applications that are fundamentally not even possible with noble metal nanoparticles. Realization of these promises will rely on the materials chemistry becoming more robust and also on multidisciplinary efforts at fabrication and characterization of test devices. The field of semiconductor LSPRs is young but fraught with tremendous excitement and activity for chemists, optical physicists, and device engineers alike.

## ■ AUTHOR INFORMATION

### Corresponding Author

\*E-mail: jain@illinois.edu.

### Notes

The authors declare no competing financial interest.

### Biographies

Jacob A. Fauchaux is a NSF Graduate Fellow working in the Jain lab at UIUC. He graduated *summa cum laude* from Louisiana Tech University with a B.S. in Chemistry in 2012. His research interests include plasmons in semiconductors and heterostructures.



**Alexandria L. D. Stanton** is a NSF Graduate Fellow and UIUC Graduate College Distinguished Fellow working for Prashant K. Jain at UIUC. She graduated from the University of Arizona with a B.S. in Chemistry in 2012. She is investigating plasmons sustained by small numbers of carriers in semiconductor nanocrystals.

**Prashant K. Jain** is an Assistant Professor of Chemistry at UIUC with research interests in nano-optics, catalysis, and solid-state transitions, areas in which he and his group (<http://nanogold.org>) have published over 40 papers that have been cited over 7000 times. His finding of plasmon resonances in semiconductor nanocrystals has been recognized by MIT's TR35 and at Google Solve for X.

## ■ ACKNOWLEDGMENTS

This material is based upon work supported by the National Science Foundation Graduate Research Fellowship Program (J.A.F. and A.L.D.S.) under Grant No. DGE-1144245. P.K.J. acknowledges support from the DuPont Young Professor Award.

## ■ REFERENCES

- (1) Kneipp, K.; Wang, Y.; Kneipp, H.; Perelman, L.; Itzkan, I.; Dasari, R.; Feld, M. Single Molecule Detection Using Surface-Enhanced Raman Scattering (SERS). *Phys. Rev. Lett.* **1997**, *78*, 1667–1670.
- (2) Nie, S.; Emory, S. Probing Single Molecules and Single Nanoparticles by Surface-Enhanced Raman Scattering. *Science* **1997**, *275*, 1102–1106.
- (3) Dieringer, J. A.; Wustholz, K. L.; Masiello, D. J.; Camden, J. P.; Kleinman, S. L.; Schatz, G. C.; Van Duyne, R. P. Surface-Enhanced Raman Excitation Spectroscopy of a Single Rhodamine 6G Molecule. *J. Am. Chem. Soc.* **2009**, *131*, 849–854.
- (4) Willets, K. A.; Stranahan, S. M.; Weber, M. L. Shedding Light on Surface-Enhanced Raman Scattering Hot Spots through Single-Molecule Super-Resolution Imaging. *J. Phys. Chem. Lett.* **2012**, *3*, 1286–1294.
- (5) Larsson, E. M.; Langhammer, C.; Zorić, I.; Kasemo, B. Nanoplasmonic Probes of Catalytic Reactions. *Science* **2009**, *326*, 1091–1094.
- (6) Rosman, C.; Prasad, J.; Neiser, A.; Henkel, A.; Edgar, J.; Sönnichsen, C. Multiplexed Plasmon Sensor for Rapid Label-Free Analyte Detection. *Nano Lett.* **2013**, *13*, 3243–3247.
- (7) Redmond, P. L.; Wu, X.; Brus, L. Photovoltage and Photocatalyzed Growth in Citrate-Stabilized Colloidal Silver Nanocrystals. *J. Phys. Chem. C* **2007**, *111*, 8942–8947.
- (8) Liu, N.; Langguth, L.; Weiss, T.; Kätzel, J.; Fleischhauer, M.; Pfau, T.; Giessen, H. Plasmonic Analogue of Electromagnetically Induced Transparency at the Drude Damping Limit. *Nat. Mater.* **2009**, *8*, 758–762.
- (9) Zhao, Y.; Pan, H.; Lou, Y.; Qiu, X.; Zhu, J.; Burda, C. Plasmonic Cu<sub>(2-x)</sub>S Nanocrystals: Optical and Structural Properties of Copper-Deficient Copper(I) Sulfides. *J. Am. Chem. Soc.* **2009**, *131*, 4253–4261.
- (10) Luther, J. M.; Jain, P. K.; Ewers, T.; Alivisatos, A. P. Localized Surface Plasmon Resonances Arising from Free Carriers in Doped Quantum Dots. *Nat. Mater.* **2011**, *10*, 361–366.
- (11) Routzahn, A. L.; White, S. L.; Fong, L.-K.; Jain, P. K. Plasmonics with Doped Quantum Dots. *Isr. J. Chem.* **2012**, *52*, 983–991.
- (12) Dorfs, D.; Härtling, T.; Misztal, K.; Bigall, N. C.; Kim, M. R.; Genovese, A.; Falqui, A.; Povia, M.; Manna, L. Reversible Tunability of the Near-Infrared Valence Band Plasmon Resonance in Cu<sub>(2-x)</sub>Se Nanocrystals. *J. Am. Chem. Soc.* **2011**, *133*, 11175–11180.
- (13) Valle, G.; Della Scotognella, F.; Ram, A.; Kandada, S.; Zavelani-rossi, M.; Li, H.; Conforti, M.; Longhi, S.; Manna, L.; Lanzani, G.; et al. Ultrafast Optical Mapping of Nonlinear Plasmon Dynamics in Cu<sub>2-x</sub>Se Nanoparticles. *J. Phys. Chem. Lett.* **2013**, *4*, 3337–3344.
- (14) Manthiram, K.; Alivisatos, A. P. Tunable Localized Surface Plasmon Resonances in Tungsten Oxide Nanocrystals. *J. Am. Chem. Soc.* **2012**, *134*, 3995–3998.
- (15) Garcia, G.; Buonsanti, R.; Runnerstrom, E. L.; Mendelsberg, R. J.; Llordes, A.; Anders, A.; Richardson, T. J.; Milliron, D. J. Dynamically Modulating the Surface Plasmon Resonance of Doped Semiconductor Nanocrystals. *Nano Lett.* **2011**, *11*, 4415–4420.
- (16) Kriegel, I.; Rodríguez-Fernández, J.; Wisnet, A.; Zhang, H.; Waurisch, C.; Eychmüller, A.; Dubavik, A.; Govorov, A. O.; Feldmann, J. Shedding Light on Vacancy-Doped Copper Chalcogenides: Shape-Controlled Synthesis, Optical Properties, and Modeling of Copper Telluride Nanocrystals with Near-Infrared Plasmon Resonances. *ACS Nano* **2013**, *7*, 4367–4377.
- (17) Yang, H.; Chen, C.; Yuan, F.; Tuan, H. Designed Synthesis of Solid and Hollow Cu<sub>2-x</sub>Te Nanocrystals with Tunable Near-Infrared Localized Surface Plasmon Resonance. *J. Phys. Chem. C* **2013**, *117*, 21955–21964.
- (18) Polking, M. J.; Jain, P. K.; Bekenstein, Y.; Banin, U.; Millo, O.; Ramesh, R.; Alivisatos, A. P. Controlling Localized Surface Plasmon Resonances in GeTe Nanoparticles Using an Amorphous-to-Crystalline Phase Transition. *Phys. Rev. Lett.* **2013**, *111*, 037401.
- (19) Fauchaux, J. A.; Jain, P. K. Plasmons in Photocharged ZnO Nanocrystals Revealing the Nature of Charge Dynamics. *J. Phys. Chem. Lett.* **2013**, *4*, 3024–3030.
- (20) Buonsanti, R.; Llordes, A.; Aloni, S.; Helms, B. A.; Milliron, D. J. Tunable Infrared Absorption and Visible Transparency of Colloidal Aluminum-Doped Zinc Oxide Nanocrystals. *Nano Lett.* **2011**, *11*, 4706–4710.
- (21) Schimpf, A. M.; Thakkar, N.; Gunthardt, C. E.; Masiello, D. J.; Gamelin, D. R. Charge-Tunable Quantum Plasmons in Colloidal Semiconductor Nanocrystals. *ACS Nano* **2013**, *8*, 1065–1072.
- (22) Kelly, K. L.; Coronado, E.; Zhao, L. L.; Schatz, G. C. The Optical Properties of Metal Nanoparticles: The Influence of Size, Shape, and Dielectric Environment. *J. Phys. Chem. B* **2003**, *107*, 668–677.
- (23) Hooshmand, N.; Jain, P. K.; El-Sayed, M. A. Plasmonic Spheroidal Metal Nanoshells Showing Larger Tunability and Stronger Near Fields Than Their Spherical Counterparts: An Effect of Enhanced Plasmon Coupling. *J. Phys. Chem. Lett.* **2011**, *2*, 374–378.
- (24) Zhang, J. Z.; Noguez, C. Plasmonic Optical Properties and Applications of Metal Nanostructures. *Plasmonics* **2008**, *3*, 127–150.
- (25) Slaughter, L.; Chang, W.-S.; Link, S. Characterizing Plasmons in Nanoparticles and Their Assemblies with Single Particle Spectroscopy. *J. Phys. Chem. Lett.* **2011**, *2*, 2015–2023.
- (26) Hirakawa, T.; Kamat, P. V. Charge Separation and Catalytic Activity of Ag@TiO<sub>2</sub> Core–Shell Composite Clusters under UV-Irradiation. *J. Am. Chem. Soc.* **2005**, *127*, 3928–3934.
- (27) Novo, C.; Funston, A. M.; Mulvaney, P. Direct Observation of Chemical Reactions on Single Gold Nanocrystals Using Surface Plasmon Spectroscopy. *Nat. Nanotechnol.* **2008**, *3*, 598–602.
- (28) Chikan, V. Challenges and Prospects of Electronic Doping of Colloidal Quantum. *J. Phys. Chem. Lett.* **2011**, *2*, 2783–2789.
- (29) Ruddy, D. A.; Erslev, P. T.; Habas, S. E.; Seabold, J. A.; Neale, N. R. Surface Chemistry Exchange of Alloyed Germanium Nanocrystals: A Pathway toward Conductive Group IV Nanocrystal Films. *J. Phys. Chem. Lett.* **2013**, *4*, 416–421.
- (30) Jain, P. K.; Manthiram, K.; Engel, J. H.; White, S. L.; Fauchaux, J. A.; Alivisatos, A. P. Doped Nanocrystals as Plasmonic Probes of Redox Chemistry. *Angew. Chem., Int. Ed.* **2013**, *52*, 13671–13675.
- (31) Wei, T.; Liu, Y.; Dong, W.; Zhang, Y.; Huang, C.; Sun, Y.; Chen, X.; Dai, N. Surface-Dependent Localized Surface Plasmon Resonances in CuS Nanodisks. *ACS Appl. Mater. Interfaces* **2013**, *5*, 10473–10477.
- (32) Jain, P. K.; El-Sayed, M. A. Surface Plasmon Resonance Sensitivity of Metal Nanostructures: Physical Basis and Universal Scaling in Metal Nanoshells. *J. Phys. Chem. C* **2007**, *111*, 17451–17454.
- (33) Haes, A. J.; Zou, S.; Schatz, G. C.; Van Duyne, R. P. A Nanoscale Optical Biosensor: The Long Range Distance Dependence

of the Localized Surface Plasmon Resonance of Noble Metal Nanoparticles. *J. Phys. Chem. B* **2004**, *108*, 109–116.

(34) McFarland, A. D.; Van Duyne, R. P. Single Silver Nanoparticles as Real-Time Optical Sensors with Zeptomole Sensitivity. *Nano Lett.* **2003**, *3*, 1057–1062.

(35) Tam, F.; Moran, C.; Halas, N. Geometrical Parameters Controlling Sensitivity of Nanoshell Plasmon Resonances to Changes in Dielectric Environment. *J. Phys. Chem. B* **2004**, *108*, 17290–17294.

(36) Haberland, H.; von Issendorff, B.; Yufeng, J.; Kolar, T. Transition to Plasmonlike Absorption in Small Hg Clusters. *Phys. Rev. Lett.* **1992**, *69*, 3212–3215.

(37) Kreibig, U.; Saarländes, V. Optical Absorption of Small Metallic Particles. *Surf. Sci.* **1985**, *156*, 678–700.

(38) Scholl, J. A.; Koh, A. L.; Dionne, J. A. Quantum Plasmon Resonances of Individual Metallic Nanoparticles. *Nature* **2012**, *483*, 421–427.

(39) Haberland, H. Looking from Both Sides. *Nature* **2013**, *494*, E1–2.

(40) Guyot-Sionnest, P. Electrical Transport in Colloidal Quantum Dot Films. *J. Phys. Chem. Lett.* **2012**, *3*, 1169–1175.

(41) Shim, M.; Guyot-Sionnest, P. Organic-Capped ZnO Nanocrystals: Synthesis and n-Type Character. *J. Am. Chem. Soc.* **2001**, *123*, 11651–11654.

(42) Schimpf, A. M.; Gunthardt, C. E.; Rinehart, J. D.; Mayer, J. M.; Gamelin, D. R. Controlling Carrier Densities in Photochemically Reduced Colloidal ZnO Nanocrystals: Size Dependence and Role of the Hole Quencher. *J. Am. Chem. Soc.* **2013**, *135*, 16569–16577.

(43) Cohn, A. W.; Janßen, N.; Mayer, J. M.; Gamelin, D. R. Photocharging ZnO Nanocrystals: Picosecond Hole Capture, Electron Accumulation, and Auger Recombination. *J. Phys. Chem. C* **2012**, *116*, 20633–20642.

(44) Aruda, K. O.; Tagliazucchi, M.; Sweeney, C. M.; Hannah, D. C.; Weiss, E. A. The Role of Interfacial Charge Transfer-Type Interactions in the Decay of Plasmon Excitations in Metal Nanoparticles. *Phys. Chem. Chem. Phys.* **2013**, *15*, 7441–7449.

(45) Hou, W.; Cronin, S. B. A Review of Surface Plasmon Resonance-Enhanced Photocatalysis. *Adv. Funct. Mater.* **2013**, *23*, 1612–1619.

(46) Nishijima, Y.; Ueno, K.; Yokota, Y.; Murakoshi, K.; Misawa, H. Plasmon-Assisted Photocurrent Generation from Visible to Near-Infrared Wavelength Using a Au-Nanorods/TiO<sub>2</sub> Electrode. *J. Phys. Chem. Lett.* **2010**, *1*, 2031–2036.

(47) Kamat, P. V.; Patrick, B. Photophysics and Photochemistry of Quantized ZnO Colloids. *J. Phys. Chem.* **1992**, *96*, 6829–6834.

(48) Subramanian, V.; Wolf, E. E.; Kamat, P. V. Green Emission to Probe Photoinduced Charging Events in ZnO–Au Nanoparticles. *J. Phys. Chem. B* **2003**, *107*, 7479–7485.

(49) Jain, P. K.; Huang, W.; El-Sayed, M. A. On the Universal Scaling Behavior of the Distance Decay of Plasmon Coupling in Metal Nanoparticle Pairs: A Plasmon Ruler Equation. *Nano Lett.* **2007**, *7*, 2080–2088.

(50) Jain, P. K.; Eustis, S.; El-Sayed, M. A. Plasmon Coupling in Nanorod Assemblies: Optical Absorption, Discrete Dipole Approximation Simulation, and Exciton-Coupling Model. *J. Phys. Chem. B* **2006**, *110*, 18243–18253.

(51) Chen, T.; Pourmand, M.; Feizpour, A.; Cushman, B.; Reinhard, B. M. Tailoring Plasmon Coupling in Self-Assembled One-Dimensional Au Nanoparticle Chains through Simultaneous Control of Size and Gap Separation. *J. Phys. Chem. Lett.* **2013**, *4*, 2147–2152.

(52) Hsu, S.-W.; On, K.; Tao, A. R. Localized Surface Plasmon Resonances of Anisotropic Semiconductor Nanocrystals. *J. Am. Chem. Soc.* **2011**, *133*, 19072–19075.

(53) Hsu, S.; Bryks, W.; Tao, A. R. Effects of Carrier Density and Shape on the Localized Surface Plasmon Resonances of Cu<sub>2–x</sub>S Nanodisks. *Chem. Mater.* **2012**, *24*, 3765–3771.

(54) Mendelsberg, R. J.; Garcia, G.; Li, H.; Manna, L.; Milliron, D. J. Understanding the Plasmon Resonance in Ensembles of Degenerately Doped Semiconductor Nanocrystals. *J. Phys. Chem. C* **2012**, *116*, 12226–12231.

(55) Frederick, M. T.; Amin, V. A.; Weiss, E. A. Optical Properties of Strongly Coupled Quantum Dot–Ligand Systems. *J. Phys. Chem. Lett.* **2013**, *4*, 634–640.

(56) Schlather, A. E.; Large, N.; Urban, A. S.; Nordlander, P.; Halas, N. J. Near-Field Mediated Plexcitonic Coupling and Giant Rabi Splitting in Individual Metallic Dimers. *Nano Lett.* **2013**, *13*, 3281–3286.

(57) Manjavacas, A.; García de Abajo, F. J.; Nordlander, P. Quantum Plexcitonics: Strongly Interacting Plasmons and Excitons. *Nano Lett.* **2011**, *11*, 2318–2323.

(58) Tiggesbaumer, J.; Koller, L.; Liebsch, A.; Meiwes-Broer, K.-H. Blue Shift of the Mie Plasma Frequency in Ag Clusters and Particles. *Phys. Rev. A* **1993**, *48*, 1749–1752.